Model Predictive Control Strategy of Grid-Tied Converter Control in Weak-Grid Conditions for Containerized Microgrid (CMG) Systems

Gaurav Gupta, Suman Mondal and Ali Maswood

August 3, 2022

Model Predictive Control Strategy of Grid-tied Converter control in Weak-Grid conditions for Containerized Microgrid (CMG) Systems

Abstract—**This paper aims to present a novel approach to design a model predictive controller (MPC) strategy for 3-phase 2-level grid connected inverters in weak-grid conditions particularly for renewable based system with solar and battery energy storage. The proposed control strategy uses a predictive current control methodology to control the decoupled grid currents by predicting the switching states of the devices, which in turn control the power fed to grid while discharging and vice-versa. The MPC essentially a variable switching modulation strategy can excite the output filter near it's corner frequency, therefore resonance effect can observe and introduces lower order harmonics in output voltage and current. This paper propose a mitigation strategy for the resonance effect in LCL filter. The proposed active damping strategy doesn't compromise the dynamic performance of the power control of grid-tied inverters.**

Index Terms—**microgrids, renewable energy resources, model predictive control.**

I. Introduction

In recent few years, the model predictive control (MPC) algorithms have been widely implemented in several modified forms in many industrial applications. Using predictive control method it is possible to avoid the cascaded structure which is typically used in a linear control scheme, also it is best suited when the requirement is to obtain very fast transient responses. The Finite Control Set (FCS)-MPC has a natural and effective algorithm for controlling power converters, without implementing PI controllers and modulators [1].

For using particularly in renewable based systems MPC can be a potential option for fast and efficient dynamic control of power and frequency over different kinds of system disturbances and load fluctuations in weak-grid conditions, which is usually encountered in remote areas. Model predictive control can handle multiple-input multiple-output (MIMO) systems easily, non-linearities in the system can be easily handled, also it allows imposition of constraints on the system.

The MPC has been successfully applied for controlling power converters in different types of power converters in past. In [2], the MPC was applied to the low voltage ride-through (LVRT) of photovoltaic (PV) power plants to improve the transient stability of PV power plants. In [3], a optimized FCS-MPC strategy for controlling a nine-level CSC converter has been proposed, a control strategy for reduction of grid current THD and voltages of DC-link capacitors is realized. In [4], a FCS-MPC control strategy using extended voltage vectors for 2-level three phase grid connected converters have been proposed, it uses simplified MPC strategy and multiple extended voltage vectors to reduce ripple in grid current. In [5], authors have followed a modified model predictive control approach to control highly-efficient and reliable inverter concept (HERIC) inverters used in photovoltaic applications, a reduction is THD is also possible due to an increase in number of switching states using virtual vectors. In [6], the authors have used FCS-MPC for complex energy systems for large scale wind power power systems. In [7], authors have presented a constant frequency FCS-MPC strategy to control the quality of output current in a grid-tied photovoltaic inverter.

In this work, a model predictive control strategy for weak-grid systems is proposed, this strategy includes synchronization algorithm as well as active damping strategy that is essential for grid/off grid inverter control framework. This control framework can also be used for a standalone system without changing the MPC core structure. The control algorithm work satisfactorily for higher renewable penetration and low X/R grid systems. The proposed MPC framework is simplified to utilize DC Bus maximum, which also allows us more reactive power handling capability without affecting the dynamics of the system performance.

II. System Control Architecture for proposed Model Predictive Control algorithm

The controller is designed in a cascaded way with the current reference calculation blocks providing references to MPC algorithm. In a grid-tied inverter synchronization of inverter with grid is necessary before closing the grid breaker. The fast synchronisation is essential for plug and play power architecture. The transient in synchronisation process may lead to reverse power flow from grid to DC Source and may lead to over-voltage on DC side or trip the overall system for some renewable resource. Here, a separate synchronization block is used for achieving synchronization as including synchronization algorithm in MPC block may lead to instability of system and increase the complexity of control framework. For synchronization purpose inverter use sensed grid voltage and capacitor voltage in stationary reference frame. The cross

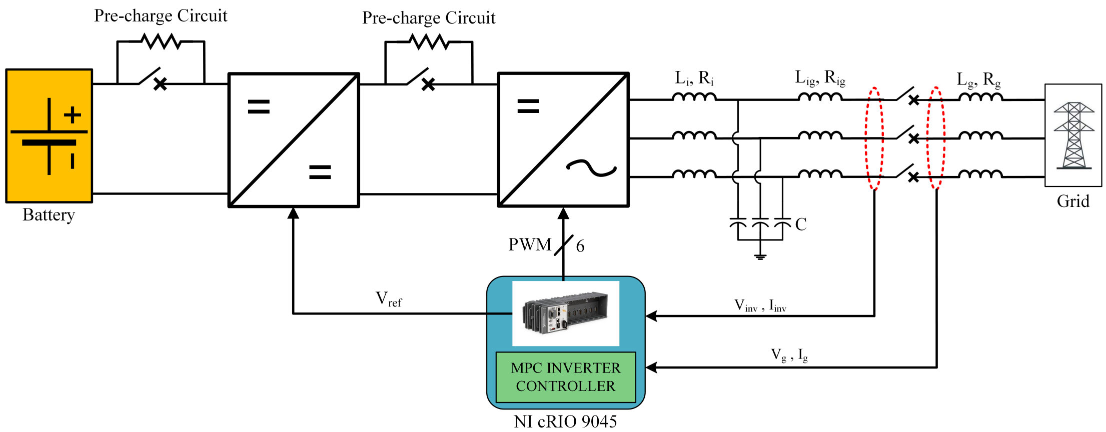

Fig. 1: Schematic used for validation of proposed control strategy

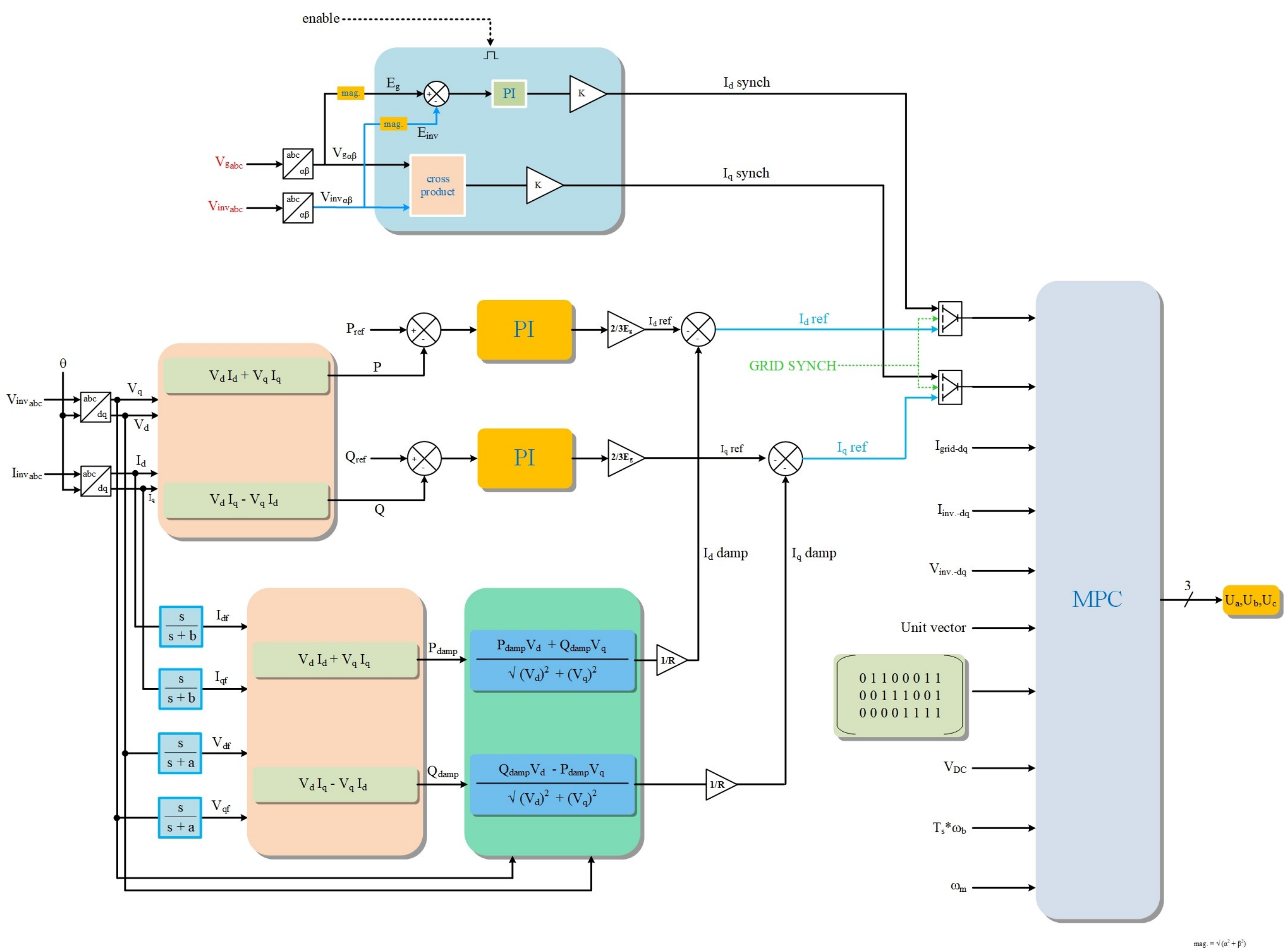

Fig. 2: Proposed cascaded structure control framework

product of the two voltages will generate the $I_{q_{synch}}$ and a PI controller from their magnitude error component can give $I_{d_{synch}}$ as shown in (1a) and (1b). A 3-ϕ PLL is also used for the grid voltage phase and frequency measurement purpose.

$$I_{d_{synch}} = K \cdot \left(K_p \cdot (E_g - E_i) + K_i \int (E_g - E_i) \right) \quad (1a)$$

$$I_{q_{synch}} = K \cdot \left(V_{g_\alpha} \otimes V_{i_\beta} + V_{i_\alpha} \otimes V_{g_\beta} \right) \quad (1b)$$

where,

$$E_g = \sqrt{V_{g_\alpha}^2 + V_{g_\beta}^2} \quad \text{and} \quad E_i = \sqrt{V_{i_\alpha}^2 + V_{i_\beta}^2}$$

After synchronization the controller use current references $I_{d_{ref}}$ and $I_{q_{ref}}$ respectively which are generated from PI controllers as given in (2a) and (2b). A pair of PI controller has been used to generate $I_{d_{ref}}$ and $I_{q_{ref}}$,

$$I_{d_{ref}} = \frac{2}{3} \cdot \frac{1}{\sqrt{V_{g_\alpha}^2 + V_{g_\beta}^2}} \cdot \left(K_p \cdot \Delta P + K_i \int \Delta P\right) \quad (2a)$$

$$I_{q_{ref}} = \frac{2}{3} \cdot \frac{1}{\sqrt{V_{g_\alpha}^2 + V_{g_\beta}^2}} \cdot \left(K_p \cdot \Delta Q + K_i \int \Delta Q\right) \quad (2b)$$

where $\Delta P = P_{ref} - P_{actual}$ and $\Delta Q = Q_{ref} - Q_{actual}$. where P_{actual} and Q_{actual} are given by,

$$P_{actual} = V_{g_d}\ I_{g_d} + V_{g_q}\ I_{g_q} \quad (3a)$$

$$Q_{actual} = V_{g_d}\ I_{g_q} - V_{g_q}\ I_{g_d} \quad (3b)$$

Power reference P_{ref} for standalone mode of operation can be calculated as,

$$P_{ref} = K_d \cdot (V_{g_{\alpha\beta}} \otimes U) \cdot \left(\frac{k}{s+k}\right) \quad (4)$$

III. Modelling of predictive control design

For current control in MPC structure, the output filter need to model in discrete domain and can be represented by (7) using (5) and (6). The actual state variables and current references can be represented by (8) and (9).

$$A_f = \begin{pmatrix} -\frac{R}{L} & \omega & 0 & 0 & -\frac{1}{L} & 0 \\ -\omega & -\frac{R}{L} & 0 & 0 & 0 & -\frac{1}{L} \\ 0 & 0 & -\frac{R_g}{L_g} & \omega & \frac{1}{L_g} & 0 \\ 0 & 0 & -\omega & -\frac{R_g}{L_g} & 0 & \frac{1}{L_g} \\ \frac{1}{C} & 0 & -\frac{1}{C} & 0 & \omega & 0 \\ 0 & \frac{1}{C} & 0 & -\frac{1}{C} & 0 & -\omega \end{pmatrix} \quad (5)$$

$$A_{f_e} = 6 \times 6 \quad [I] \quad (6)$$

where I is identity matrix

$$A_{f_e} = A_{f_e} + A_f \cdot T_s \quad (7)$$

$$X = \begin{pmatrix} I_{i\alpha} & I_{i\beta} & I_{g\alpha} & I_{g\beta} & V_{i\alpha} & V_{i\beta} \end{pmatrix}^T \quad (8)$$

$$X_{ref} = \begin{pmatrix} I_{d_{ref}} & I_{q_{ref}} & 0 & 0 & 0 & 0 \end{pmatrix}^T \quad (9)$$

The feedback gain for the MPC controller can be formulated by (10) after simplification.

$$K_d = A_{f_e} \cdot \begin{pmatrix} L/T_s & 0 & 0 & 0 & 0 & 0 \\ 0 & L/T_s & 0 & 0 & 0 & 0 \end{pmatrix} \quad (10)$$

The voltage vector to track the current references can calculated using (11) and corresponding error for each selected voltage vector can be calculated from (12a). The modulus of voltage error can be calculated by (12b).

$$V_{opt} = K_d \cdot (X_{ref} - X) \quad (11)$$

$$X_e = V_{opt} - M \cdot D \cdot U \quad (12a)$$

$$error = X_e \cdot {X_e}^T \quad (12b)$$

where,

$$D = \frac{2}{3} \cdot \begin{pmatrix} 1 & -\frac{1}{2} & -\frac{1}{2} \\ 0 & \frac{\sqrt{3}}{2} & -\frac{\sqrt{3}}{2} \end{pmatrix} \quad (13)$$

$$M = \begin{pmatrix} cos\theta & sin\theta \\ -sin\theta & cos\theta \end{pmatrix} \quad (14)$$

IV. Active Damping strategy for LCL filters for grid-tied inverters

To filter out the switching frequency harmonics from power line generally we use the filter with the corner frequency in the range of 1/10th of the average switching frequency of the inverter. For a 10kHz inverter with MPC the switching frequency can be as low as near the corner frequency of the filter, for our case we observe it's reaches near 1kHz. So the variable switching frequency modulation strategy like MPC architecture, inverter filter can be excited by the PWM switching. For damping the resonance from the power circuit the most simple method is passive damping by using resistive component in the circuit. But the passive method is lossy and can not be used for high power application[8]. Key idea of active damping is to remove resonance effect from inverter output voltage and current by using the inverter controller without resistive elements. Here in the proposed active damping strategy we use the sensed capacitor voltage and inverter current input as feedback for the damping loop. From voltage and power information we filter out the harmonic components. For weak-grid conditions usually the power control is realized by controlling the I_d and I_q component of the grid current as compared to conventional power control strategy where only I_d is controlled to realize power control as given in (15). The references from active damping algorithm in (17a) and (17b are added to current references from PI controllers to produce actual current references given as (2a) and (2b).

$$I_{dq_f} = \left(\frac{s}{s+a}\right) I_{inv_{dq}} \quad V_{dq_f} = \left(\frac{1}{1+b}\right) I_{inv_{dq}} \quad (15)$$

The damped power outputs signals are,

$$P_{damp} = V_{d_f}\ I_{d_f} + V_{q_f}\ I_{q_f} \quad (16a)$$

$$Q_{damp} = V_{d_f}\ I_{q_f} - V_{q_f}\ I_{d_f} \quad (16b)$$

Eventually, $I_{d_{damp}}$ and $I_{q_{damp}}$ are calculated as,

$$I_{d_{damp}} = \frac{V_{i_d}\ P_{damp} + V_{i_q}\ Q_{damp}}{\sqrt{V_{i_d}^2 + V_{i_q}^2}} \quad (17a)$$

$$I_{q_{damp}} = \frac{V_{i_q}\ P_{damp} - V_{i_d}\ Q_{damp}}{\sqrt{V_{i_d}^2 + V_{i_q}^2}} \quad (17b)$$

The reference signals fed to controller are,

$$I_{dq_{ref}} = I_{dq_{damp}} + I_{dq_{actual}} \quad (18)$$

Constants a and b used for this work are 300 and 30 respectively.

V. Simulation results of proposed Model Predictive Control

For this work we have used a battery fed 3-phase 2-level VSI connected to grid through a LCL filter and breaker. For cHIL validation, OP4510 real time simulator, powered by Kintex-7 FPGA kit from OPAL-RT has been used for real time simulations. The plant is modelling in done in Simulink environment using 3-phase VSI block from RTE Drive blockset, which uses FPGA. For PWM generation purpose, event generator and detector blocks from RT Events blockset which support generation and acquisition of accurately time-stamped signals. The MPC controller is modelled in Simulink environment using a MATLAB function block. The model parameters used for the real-time simulation are tabulated in Table I. The schematic of experimental setup used for this study has been represented in Fig. 1. Initially the model and MPC controller are validated in offline simulation and then validated in cHIL(controller-hardware-in-loop). The results of simulation with active damping strategy are plotted in Fig. 6 and Fig. 7.

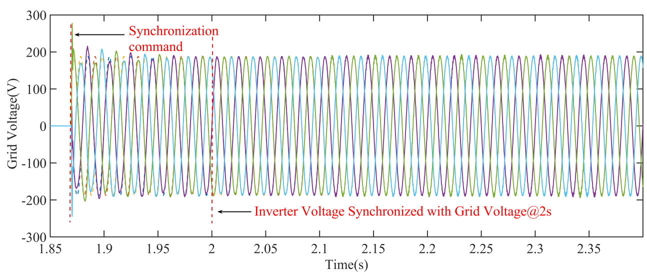

(a)

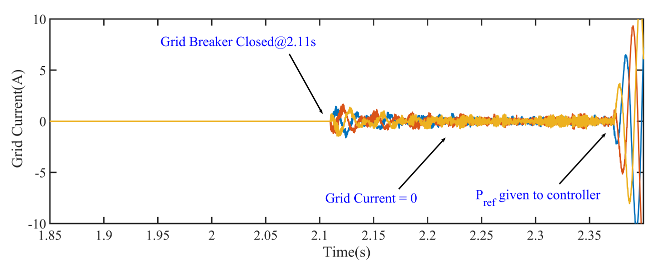

(b)

Fig. 3: Grid/Inverter Voltage and Current after enabling grid-synchronization command

The results show that the MPC control framework can synchronize within short time with the grid after synchronization command is enabled. After inverter is synchronized with the grid, and power setpoint can be given, it is evident from results that proposed predictive control achieves the referenced power setpoints within short time with a negligible over-shoot. The active damping strategy works satisfactorily with the predictive control to eliminate the low order harmonics present as a result of resonance at corner frequency in the LCL filter. This is also demonstrated through results in Fig. 7 and Fig. 8. The sampling time used for this real-time simulation is 10μs. The average switching frequency for the controller reaches near 10kHz during simulation. For this work no dead time has been used for switching devices.

Electrical Parameters	**Value**
Rated Power	10 kW
LCL Filter Inductance(L_1)	3 mH
LCL Filter Resistance(R_1)	0.5 Ω
LCL Filter Inductance(L_2)	0.01 mH
LCL Filter Resistance(R_2)	0.1 mH
Filter Capacitance(C_1)	10 µF
Grid Side Inductance(L_g)	1 mH
Grid Side Resistance(R_g)	0.1 Ω
Switching Frequency	10 kHz
Sampling Time(T_s)	10 µs

TABLE I: Model parameters used for the cHIL simulation

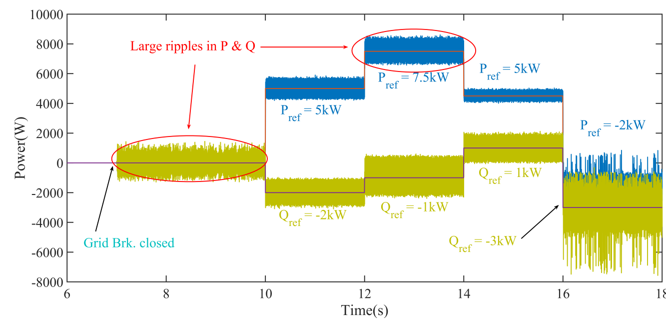

Fig. 4: Real and Reactive Power characteristics without active-damping strategy for different power setpoints

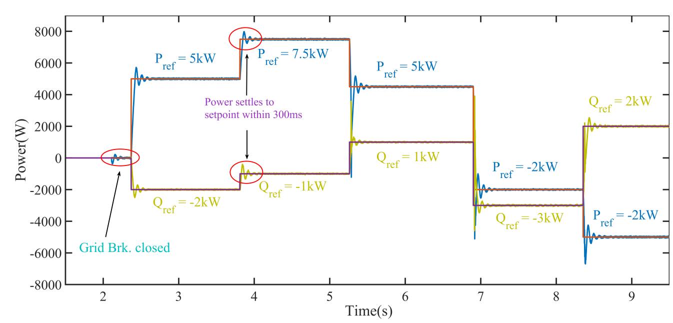

Fig. 5: Real and Reactive Power characteristics with active-damping strategy for different power setpoints

When a power command is given to controller after synchronization, the controller tries to stabilize at setpoint after small transient as shown in Fig. 6, without the presence of active damping strategy the controller follows the reference but due to the presence of harmonics the THD is high in output current which can be seen in Fig. 7.

After the controller stabilizes at previous setpoint, another setpoint of $P = 7.5\,\text{kW}$ and $Q = -1\,\text{kVAr}$ is given to controller. The transient results with active damping in Fig. 8 show better dynamic performance and lower THD than the results without damping in Fig. 7.

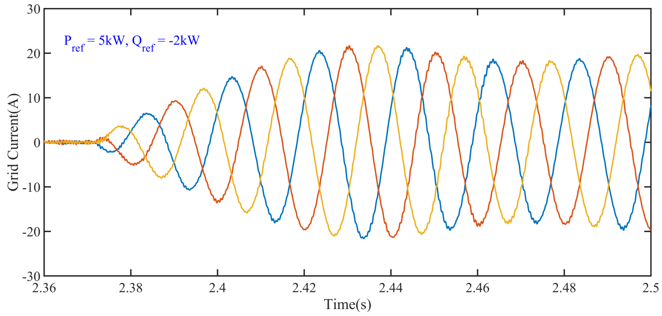

Fig. 6: Grid Current characteristics for step change from $0kW$ to $P = 5\,\mathrm{kW}$ and $Q = -2\,\mathrm{kVAr}$

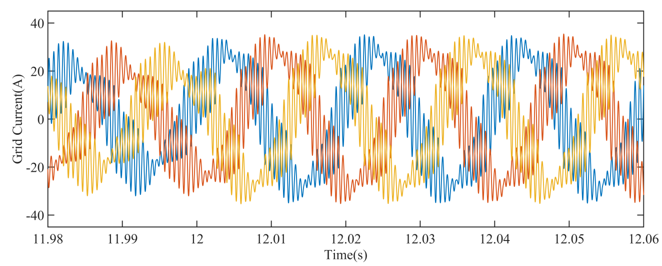

Fig. 7: Grid Current characteristics for step change from $P = 5kW$ and $Q = -2\,\mathrm{kVAr}$ to $P = 7.5kW$ and $Q = -1\,\mathrm{kVAr}$ without active damping strategy

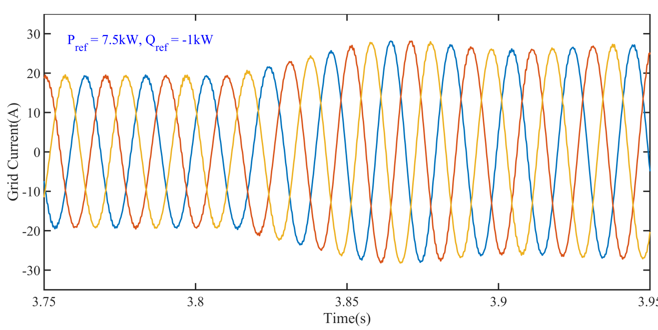

Fig. 8: Grid Current characteristics for step change from $P = 5\,\mathrm{kW}$ and $Q = -2\,\mathrm{kVAr}$ to $P = 5\,\mathrm{kW}$ and $Q = -1\,\mathrm{kVAr}$ with active damping strategy

VI. Conclusion

The results from simulation show that MPC for grid tied converters in weak grid conditions works satisfactorily with active damping strategy. The controller follows the real and reactive power command quickly without any significant disturbance in the system. Initially the power setpoint is given as $P = 5\,\mathrm{kW}$ and $Q = -2\,\mathrm{kVAr}$, after the power stabilizes at given setpoint, the power command is changed to $P = 7.5\,\mathrm{kW}$ and $Q = -1\,\mathrm{kVAr}$. Moreover from FFT analysis results it can be proved that the THD of grid current by using active damping reduces from 8.22% to 2.5%, which is within the limits given by IEEE 519-2014[9]. The proposed controller uses a novel approach to realize MPC controller for grid-tied inverters specially in weak grid conditions with active damping strategy to mitigate the effect of resonance in LCL filters.

References

[1] J. D. Barros, J. F. A. Silva, and É. G. Jesus, "Fast-predictive optimal control of npc multilevel converters," *IEEE Transactions on Industrial Electronics*, vol. 60, no. 2, pp. 619–627, 2012.

[2] G. Li, "Nonlinear model predictive control of a wave energy converter based on differential flatness parameterisation," *International Journal of Control*, vol. 90, no. 1, pp. 68–77, 2017.

[3] A. N. Alquennah, M. Trabelsi, K. Rayane, H. Vahedi, and H. Abu-Rub, "Real-time implementation of an optimized model predictive control for a 9-level csc inverter in grid-connected mode," *Sustainability*, vol. 13, no. 15, 2021, ISSN: 2071-1050. [Online]. Available: https://www.mdpi.com/2071-1050/13/15/8119.

[4] K. Alam, D. Xiao, D. Zhang, and M. Rahman, "Simplified finite control set model predictive control (fcs-mpc) with extended voltage vectors for grid connected converters," in *2017 Australasian Universities Power Engineering Conference (AUPEC)*, IEEE, 2017, pp. 1–6.

[5] E. Zangeneh Bighash, S. M. Sadeghzadeh, E. Ebrahimzadeh, and F. Blaabjerg, "High quality model predictive control for single phase grid-connected photovoltaic inverters," *Electric Power Systems Research*, vol. 158, pp. 115–125, 2018, ISSN: 0378-7796. DOI: https://doi.org/10.1016/j.epsr.2018.01.001. [Online]. Available: https://www.sciencedirect.com/science/article/pii/S0378779618300014.

[6] J.-R. Yuan, F.-F. Shen, J.-Z. Xu, C.-K. Li, and D. Wang, "Finite control set model predictive control for complex energy system with large-scale wind power," *Complexity*, 2019.

[7] Z. Zhang, B. Li, R. Ma, X. Chen, and Z. Dai, "Finite-control-set model predictive control with a constant switching frequency for single-phase grid-connected photovoltaic inverter," *IET Power Electronics*, vol. 15, no. 2, pp. 123–131, 2022. DOI: https://doi.org/10.1049/pel2.12216. eprint: https://ietresearch.onlinelibrary.wiley.com/doi/pdf/10.1049/pel2.12216. [Online]. Available: https://ietresearch.onlinelibrary.wiley.com/doi/abs/10.1049/pel2.12216.

[8] S. Mondal and D. Kastha, "Input reactive power controller with a novel active damping strategy for a matrix converter fed direct torque controlled dfig for wind power generation," *IEEE Journal of Emerging and Selected Topics in Power Electronics*, vol. 8, no. 4, pp. 3700–3711, 2020. DOI: 10.1109/JESTPE.2019.2938012.

[9] "Ieee recommended practice and requirements for harmonic control in electric power systems," *IEEE Std 519-2014 (Revision of IEEE Std 519-1992)*, pp. 1–29, 2014. DOI: 10.1109/IEEESTD.2014.6826459.